FINAL TECHNICAL PROGRESS REPORT

Award No.: DE-SC0008875

Program Manager: Dr. John Mandrekas, Program Manager, U.S. Department of Energy, Office of Fusion Energy Sciences (FES), E-mail: john.mandrekas@science.doe.gov

Recipient Institution: University of Massachusetts, Amherst

Project Title: "Plasma Surface Interactions: Bridging from the Surface to the Micron Frontier through Leadership Class Computing"

Principal Investigator: Dr. Dimitrios Maroudas, Professor
University of Massachusetts, Amherst
Department of Chemical Engineering,
154A Goessmann Laboratory, 686 North Pleasant Street, Amherst, MA 01003-9303
E-mail: maroudas@ecs.umass.edu;
Telephone: (413) 545-3617; FAX: (413) 545-1647

Report Date: December 10, 2018

Period Covered: August 15, 2012 – August 14, 2018

This is the final technical report for this 5-year research project (with a 1-year no-cost extension). This is an institutional (University of Massachusetts, Amherst) final research report for a **SciDAC** (**Sci**entific **D**iscovery through **A**dvanced **C**omputing) research project.

PSI-SciDAC UMass Amherst Final Research Report (8/15/2012 – 8/14/2018)

Prof. Dimitrios Maroudas, University of Massachusetts (UMass), Amherst, PI

Throughout the grant period, research at UMass Amherst focused on the atomic-scale analysis of the dynamics and kinetics (transport and reactions) of small mobile helium clusters (He_n, $1 \leq n \leq 7$) near surfaces and grain boundaries in plasma-exposed tungsten, as well as the proper parameterization and incorporation of these processes into our SciDAC team's continuum-level cluster dynamics code (Xolotl). Our work also included characterization of large-scale molecular-dynamics (MD) simulation results of helium implantation into tungsten based on the findings of our analysis and comparisons of Xolotl simulation predictions with the large-scale MD simulation results for Xolotl validation purposes; emphasis was placed on the impact of helium cluster dynamics/kinetics on tungsten surface morphology, near-surface tungsten structure, and helium retention. Furthermore, our work included initiation of a research program on evaluating the impact of structural defects in tungsten due to plasma exposure (such as helium nanobubbles) on tungsten's thermophysical properties, focusing on lattice thermal conductivity. Our studies contributed to a fundamental understanding of the effects of plasma-surface interactions on the dynamical response of plasma-facing materials in nuclear fusion devices and the development of predictive hierarchical multiscale computational tools for the quantitative description of the material's dynamical response to plasma exposure [1]. Our research findings are outlined here.

1. *Analysis of the Interactions of Mobile Helium Clusters with Surfaces and Grain Boundaries in Plasma-Exposed Tungsten: The Origin of Drift in Cluster Transport*

We have carried out a systematic protocol of atomistic computations for the interactions of small mobile helium clusters with free surfaces and grain boundaries (GBs) in tungsten toward development of continuum drift-diffusion-reaction models for the dynamics of mobile helium clusters in plasma-exposed tungsten. Molecular-statics (MS) simulations based on reliable many-body interatomic potentials have been conducted for He_n ($1 \leq n \leq 7$) clusters near sinks, such as surfaces, GBs, and regions in the vicinity of junctions where GBs intersect free surfaces to obtain the potential energy profiles of the He_n clusters as a function of the distance, d, of the cluster's center of mass from each sink examined. Elastic interaction potentials based on elastic inclusion theory provide an excellent description of the MS results for the cluster-sink interactions. The elastic interaction potential is expressed as $E_s(d) = -A/d^3$, where A, the key parameter in these elastic models, is the sink segregation strength; A is found to increase with increasing cluster size. Such cluster-sink interactions are responsible for the migration of small helium clusters by drift and for helium segregation on surfaces and grain boundaries in tungsten. Such helium segregation on sinks is observed in large-scale molecular-dynamics simulations of He aggregation in model polycrystalline tungsten at 933 K upon He implantation (see Section 3 of this report).

Figure 1 shows representative results from the MS computations of He_n cluster-surface interactions for clusters near the W(100) surface, in terms of an interaction energy profile, where the minimum energy of the relaxed atomic configuration is plotted as a function of the distance, d, of the He_n cluster's center of mass from the surface. At each distance from the sink (surface or grain boundary), numerous initial cluster configurations were used and local energy minimization was performed with respect to the atomic coordinates; the minimum energy in this manifold of local minima was then assigned as the energy of the relaxed atomic configuration at

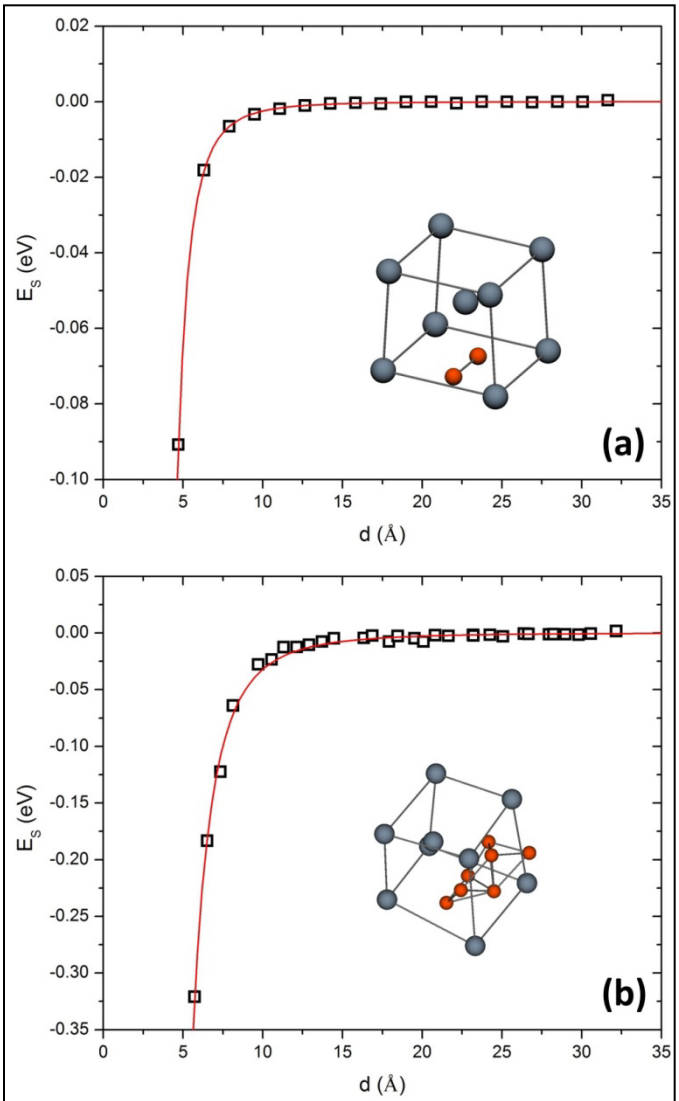

Fig. 1. Potential energy profiles (open squares), $E_s(d)$, from MS simulations for the interaction of (a) the He_2 and (b) the He_7 cluster with the W(100) surface in the near-surface region as a function of the distance d of the cluster's center of mass from the surface. The solid lines represent least-squares fits to the simulation results according to the elastic inclusion theory. The structurally relaxed cluster configurations are shown in the insets.

this distance. For the computation of each profile such as those shown in Fig. 1, 5,000-20,000 MS computations were required. The MS results show that the computed energies go asymptotically to zero in the bulk of the crystal, away from the surface, i.e., the zero energy level corresponds to the formation energy of the cluster in the bulk crystal. The results shown in Figs. 1(a) and 1(b) are for the He_2 (di-He) and the He_7 (seven-He) clusters, respectively. The corresponding relaxed cluster configurations are shown in the insets in Figs. 1(a) and 1(b) and the red solid lines represent least-squares fits to the MS results according to the elastic interaction potential from the elastic inclusion theory. It is evident that the theory provides an excellent fit to the computational results, and this is the case for all the seven clusters (He_n, $1 \leq n \leq 7$) and all the sinks that we examined; the sinks examined included the W(100), W(110), W(111), and W(211) surfaces and the $\Sigma 3\langle 111\rangle\{121\}$ symmetric tilt GB. The elastic potential well becomes deeper, i.e., the attraction to the sink becomes stronger as the cluster size n increases. This trend is elucidated further in Fig. 2, where A is plotted as a function of n for some of the sinks examined. Figure 2 shows that A(n) is generally a monotonically increasing function. The only anomaly to this monotonic increase is exhibited at n = 4, where either A(4) is lower than A(3) or the derivative dA/dn decreases locally depending on the sink. We attribute this anomaly to the cluster morphological changes undergone in the structurally relaxed configurations at sizes in the vicinity of n = 4; at n = 4, the 4 He atoms of He_4 occupy neighboring tetrahedral interstitial lattice sites forming a compact tetrahedron.

The theory of diffusional species transport with drift due to surface segregation has been described in an invited article that has been published in a special issue of *AIChE Journal* [2]. The detailed analysis of He_n cluster-sink interactions for surfaces and GBs in plasma-exposed tungsten has been published as an article in the *Journal of Applied Physics* [3].

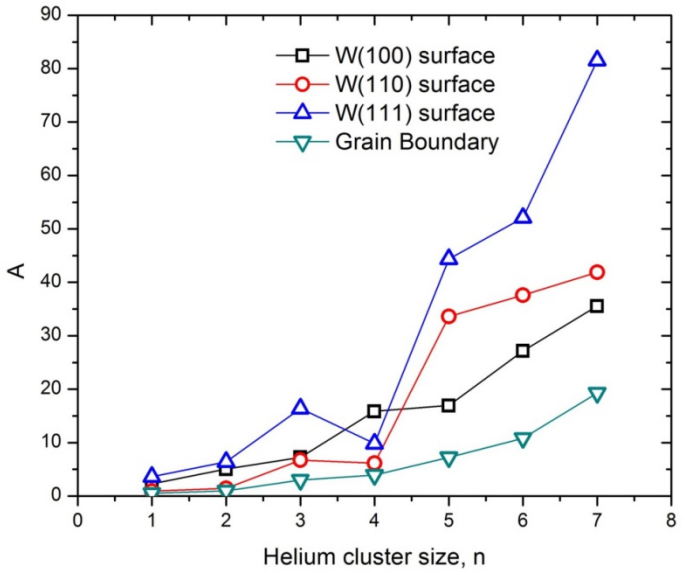

Fig. 2. Sink segregation strength, A (in eV·Å^3), for He_n cluster-sink interactions as a function of He_n cluster size, n, with sinks consisting of the W(100), W(110), and W(111) surfaces and the Σ3<111>{121} symmetric tilt grain boundary.

2. *Analysis of Small Mobile Helium Cluster Reactions near Surfaces of He-Implanted Tungsten*

We have carried out a systematic atomic-scale analysis of the dynamics of small mobile helium clusters, He_n ($1 \leq n \leq 3$), in tungsten, near tungsten surfaces, focusing on the low-Miller-index surfaces W(100), W(110), W(111), and W(211). These helium clusters are attracted to tungsten surfaces due to an elastic interaction force that drives surface segregation, as established in Section 1 of this report. The analysis was based on molecular-dynamics (MD) simulations according to state-of-the-art many-body interatomic potentials. For each cluster, we generated several hundreds of one-ns-long trajectories at two temperatures, T = 1000 K and T = 1200 K, in supercells containing N = 4000 W atoms for the W(100) surface (we used N = 5120 and 6144 for the W(110) and the W(111) surface, respectively). In each trajectory, the small He cluster in the initial configuration was placed at a distance from the surface such that the cluster feels the attractive elastic interaction with the surface, typically ~10 atomic layers below the surface plane. The stability of the resulting configurations (for a small sample of each MD simulation outcome) was confirmed by analyzing much longer MD trajectories (~100 ns). The clusters were relaxed (energy minimization) at practically the same distance from the surface plane for each MD trajectory and the trajectories were initialized randomly at each temperature. We found that as the clusters migrate toward the surface, trap mutation and cluster dissociation reactions are activated at rates higher than in the bulk. These kinetic processes are responsible for important structural, morphological, and compositional features in plasma-exposed tungsten, including surface adatoms, near-surface immobile helium-vacancy complexes, and retained helium content.

The outcomes of the MD analysis for the He_2 and He_3 clusters near W(100) are summarized in Table 1. These outcomes are the kinetic processes identified and expressed as cluster reactions in Table 1. The corresponding kinetic processes identified are trap mutation, trap mutation followed by cluster dissociation, and He desorption from the surface as $He_{(g)}$. In all cases, He desorption is caused by cluster dissociation. Trap mutation is the dominant and most important type of reaction in the near-surface region: it leads to the formation of a W vacancy (a "trap") and attachment of the He_n cluster (here, n = 2 or 3) to this vacancy to form an essentially immobile He_n-vacancy (He_n-V) complex with its center located on a lattice plane l a few layers below the surface plane together with a W surface adatom, denoted as W_s. Cluster dissociation may be complete (into two and three individual He atoms for He_2 and He_3, respectively) or partial, i.e., leaving one He atom in the material in the case of He_2 and either two or one He atom(s) in the material in the case of He_3.

Table 1. List of reactions undergone by the He_2 and He_3 clusters near the W(100) surface. The integer index l indicates the lattice plane where He_m-V complexes are formed; l = 1 corresponds to the surface plane and l increases with increasing depth below the surface. The relative probabilities for all of these reactions from analysis of MD trajectories at T = 1000 K (522 and 504 MD trajectories at n = 2 and 3, respectively) and T = 1200 K (288 and 659 MD trajectories at n = 2 and 3, respectively) also are listed.

He_n	Reaction	Relative probability (T = 1000 K)	Relative probability (T = 1200 K)
n = 2	$W + He_2 \rightarrow He_2\text{-}V(l = 4) + W_s$	0.6%	0.8%
	$W + He_2 \rightarrow He_2\text{-}V(l = 3) + W_s$	74.3%	74.2%
	$W + He_2 \rightarrow He\text{-}V(l = 3) + W_s + He_{(g)}$	4.8%	5.9%
	$W + He_2 \rightarrow W + 2\ He_{(g)}$	20.3%	19.1%
n = 3	$W + He_3 \rightarrow He_3\text{-}V(l = 5) + W_s$	12.3%	15.6%
	$W + He_3 \rightarrow He_3\text{-}V(l = 4) + W_s$	84.3%	71.7%
	$W + He_3 \rightarrow He_2\text{-}V(l = 3) + W_s + He_{(g)}$	0.2%	1.7%
	$W + He_3 \rightarrow He\text{-}V(l = 3) + W_s + 2\ He_{(g)}$	2.6%	9.9%
	$W + He_3 \rightarrow W + 3\ He_{(g)}$	0.6%	1.1%

A representative MD trajectory for the dominant chemical reaction of He_3 is shown in Fig. 3, depicting and characterizing the trap mutation reaction that forms He_3-V in the 4th layer and a W_s on the surface; the three He atoms in He_3-V are on a {111} plane. The depth evolution of all three He atoms in Fig. 3(a) shows the diffusion of the cluster that stays intact and its drift to the 4th layer, while the quenched MD trajectory in Fig. 3(b) shows the trap mutation reaction with the reactant, transition, and product states, as well as the reaction energy landscape along the optimal reaction path depicted in the insets. The reaction is exothermic, releasing 3.91 eV, with a low activation energy of 0.50 eV, which explains its high relative probability of occurrence; the reaction activation energy barriers have been computed using the climbing-image nudged elastic band (CI-NEB) method. In general, the activation energies and exothermicities of such trap mutation reactions increase with increasing cluster size n.

The analysis of He_2 and He_3 cluster reactions near W(100), W(110), and W(111) surfaces has been published as an article (Letter) in *Surface Science* [4].

3. *Large-Scale MD Simulations of He Aggregation in Near-Surface Regions of He-Implanted Tungsten*

We have designed and conducted systematic large-scale MD simulation studies of He aggregation (cluster formation) in the low-energy (~100 eV) low-temperature (933 K) regime of He implantation in tungsten matrices; these MD simulations employ state-of-the-art many-body interatomic potentials and large supercells with several million W atoms. In the MD simulations, He atoms are inserted at certain frequencies in locations in the W supercell sampled from He implantation depth distributions computed from direct MD simulations of He implantation in the prescribed regime. Our MD studies emphasize on He aggregation in the near-surface region and the resulting He bubble formation and dynamics. In addition to single-crystal tungsten matrices, targeted simulation studies have been conducted on model polycrystalline tungsten to elucidate and quantify the effects of microstructure (GBs) on He bubble formation and evolution. Important parameters in the MD studies include the surface crystallographic orientation and the GB type, GB sink strength, and GB plane orientation; MD-based systematic parametric studies have been designed and conducted (see also Section 7 of this report).

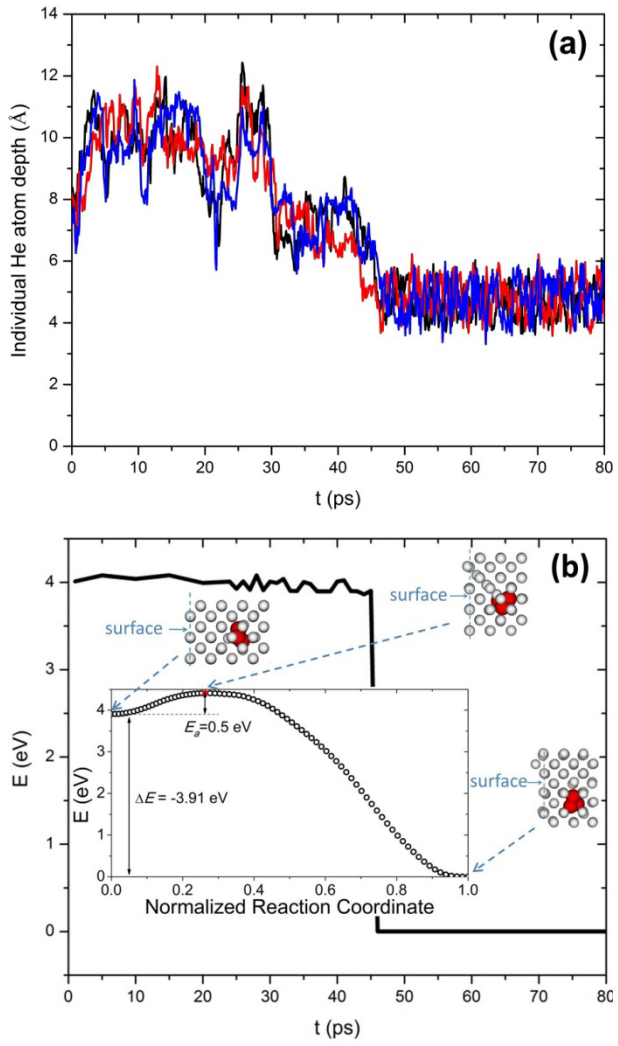

Fig. 3. Representative MD trajectory capturing the trap mutation reaction W + He_3 → He_3-V (l = 4) + W_s near W(100). (a) Evolution of depth below the surface of all three He atoms of the cluster. (b) Energy evolution along the quenched MD trajectory with the relaxed reactant-, transition-, and product-state configurations, as well as the CI-NEB-computed energy landscape of the reaction along the optimal reaction path, depicted as insets; in the inserted configurations, small silver and large red spheres denote W and He atoms, respectively.

The large-spatial-scale MD simulations of helium aggregation in model polycrystalline W reveal drift and diffusional transport of He atoms and small He_n clusters, n ≤ 7, as well as aggregate formation and growth of He bubbles; representative results from these simulations are shown in Fig. 4. The inset in Fig. 4 shows a schematic representation of the supercell used in the MD simulations with two Σ3<111>{121} symmetric tilt GBs intersecting at right angles the W(111) surface. Specifically, Fig. 4 shows the distribution of He atoms (only He atoms are shown) in the polycrystalline W model near a W{111} surface and the formation of He aggregates after 6,500 He atoms were added into the supercell model (corresponding to a simulation time of 65 ns).

The observed distribution of He atoms can be explained on the basis of the different retention and reflection rates for the W(111) surface, the rates of the mobile He_n cluster reactions, as well as the cluster-sink interactions with the surface and the GBs providing sinks that attract the mobile He_n clusters. An important reason for the high retained He content is that the trap mutation reactions (dominant cluster reactions as established in Section 2 of this report) have low energy barriers near the W(111) surface, thus resulting in a high content of substitutional He atoms near the surface. Another reason is that the W(111) surface is a strong sink for mobile He_n clusters, as we established in the study reported in Section 1 of this report. From the results of Fig. 4, it is evident that He atoms decorate the W surface and the two GBs in the near-surface region as a result of helium segregation on the surface and on the GBs due to the drift fluxes driven by the He_n cluster-surface and He_n cluster-GB interactions that we have characterized (as reported in Section 1 of this report). Very high concentrations of He are observed in the vicinity of the junctions where the GBs intersect the free surface. These observations provide further qualitative confirmation of the models of He_n cluster-sink interactions in W that we have developed. These models, in turn, aid in providing thermodynamic and kinetic interpretations to the observed He species distributions in the large-spatial-scale MD simulations.

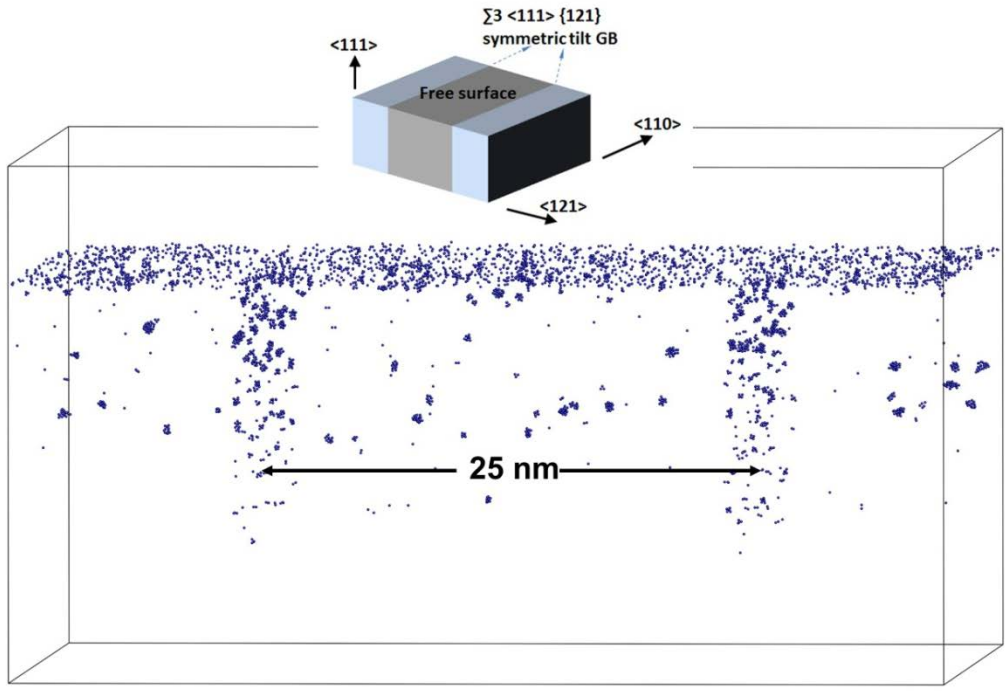

Fig. 4. Distribution of He atoms in tungsten from large-scale MD simulations of aggregation of He atoms implanted in tungsten at 933 K, using a polycrystalline tungsten model with Σ3<111>{121} symmetric tilt GBs at a distance of 25 nm from each other intersecting perpendicularly a W{111} free surface. The inset gives a schematic representation of the MD supercell used in the simulations.

Results from this work have appeared in the article on cluster-sink interactions that we have published in the *Journal of Applied Physics* [3].

4. *Helium Impurity Transport on Grain Boundaries*

We have carried out atomistic simulations, both targeted molecular-statics simulations and molecular-dynamics simulations, which show that transport of helium is inhibited on grain boundaries in tungsten. This finding is contrary to self-diffusion, or diffusion of substitutional impurities in metals, for which transport is generally enhanced along grain boundaries, but is similar to the behavior observed for hydrogen in past studies on low-angle grain boundaries, for which transport also occurs via interstitial diffusion. In the case of helium transport in tungsten, we have found that diffusion is biased toward grain boundaries, but once a helium atom or group of atoms is on a grain boundary, diffusion is impeded rather than enhanced. The reduced rate of diffusion on grain boundaries produces a higher concentration of helium in the grain boundary regions. The effect arises from the relative insolubility of helium in most materials combined with the size mismatch between helium and tungsten, which results in an interstitial diffusion mechanism rather than diffusion that relies on the presence of self-vacancies. The important implication of this study, both for a fundamental understanding of helium transport in tungsten and for analysis and interpretations of large-scale molecular-dynamics and hierarchical multi-scale simulations of helium implantation and subsequent evolution in tungsten, is that grain boundaries will not facilitate transport of helium in tungsten and other metals, and that helium is

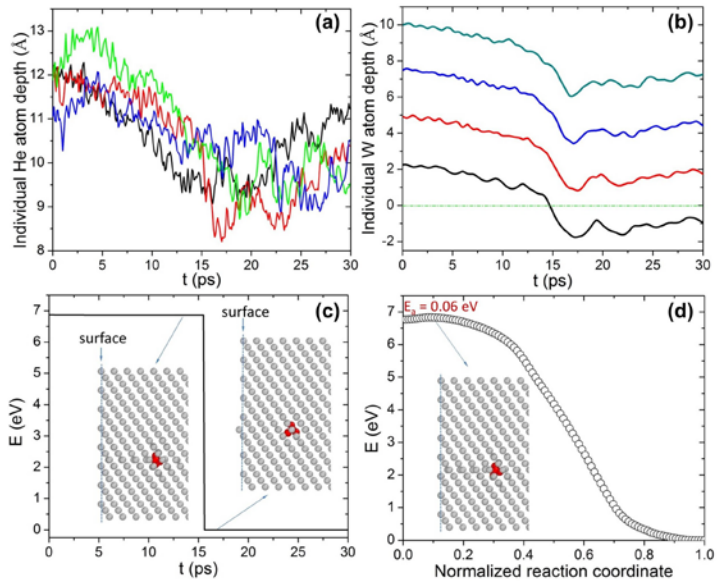

Fig. 5. Analysis of a representative MD trajectory capturing the cluster trap mutation reaction W + He_4 → He_4-V (l=12) + W_s near W(111), with the vacancy (V) forming on the 12th layer from the surface plane. (a) Evolution of depth below the surface of all four He atoms of the He_4 cluster during the trap mutation reaction. (b) Evolution of depth below the surface of the W atoms displaced substantially from their original lattice positions during the trap mutation reaction, showing the formation of one W surface adatom (W_s). (c) Energy evolution along the quenched MD trajectory during the trap mutation reaction. (d) CI-NEB-computed optimal pathway for this reaction. In the inserted configurations in (c) and (d), silver and red spheres denote W and He atoms, respectively.

in fact immobilized on grain boundaries. This work has been published as an article in *Europhysics Letters* [5].

5. *Molecular-Dynamics Analysis of Mobile Helium Cluster Reactions near Surfaces of Plasma-Exposed Tungsten*

We have conducted a systematic atomic-scale analysis of the reactions of small mobile helium clusters (He_n, $4 \leq n \leq 7$) near low-Miller-index tungsten (W) surfaces, aiming at a fundamental understanding of the near-surface dynamics of helium-carrying species in plasma-exposed tungsten. These small mobile helium clusters are attracted to the surface and migrate to the surface by Fickian diffusion and drift due to the thermodynamic driving force for surface segregation. As the clusters migrate toward the surface, trap mutation (TM) and cluster dissociation reactions are activated at rates higher than in the bulk. TM produces W adatoms and immobile complexes of helium clusters surrounding W vacancies located within the lattice planes at a short distance from the surface. These reactions have been identified and characterized in detail based on the analysis of a large number of molecular-dynamics trajectories for each such mobile cluster near W(100), W(110), W(111), and W(211) surfaces. TM is found to be the dominant cluster reaction for all cluster and surface combinations, except for the He_4 and He_5 clusters near W(100) where cluster partial dissociation following TM dominates. The optimal pathways of the reactions captured by the MD trajectories were constructed using the climbing-image nudged elastic band (CI-NEB) method and the corresponding activation energy barriers were determined. An example of analysis of a TM reaction is shown in Fig. 5. The low activation energy barriers for TM reactions near W(111) and W(110) and the higher energy barriers for PD reactions near W(110) are the reasons why TM reactions are the dominant ones for helium clusters near these two surfaces. We have found that there exists a critical cluster size, n = 4 near W(100), W(111), and W(211) and n = 5 near W(110), beyond which the formation of multiple W adatoms and vacancies in the TM reactions is observed. The identified cluster reactions are responsible for important structural, morphological, and compositional features in the plasma-exposed tungsten, including surface adatom populations, near-surface immobile helium-vacancy complexes, and retained helium

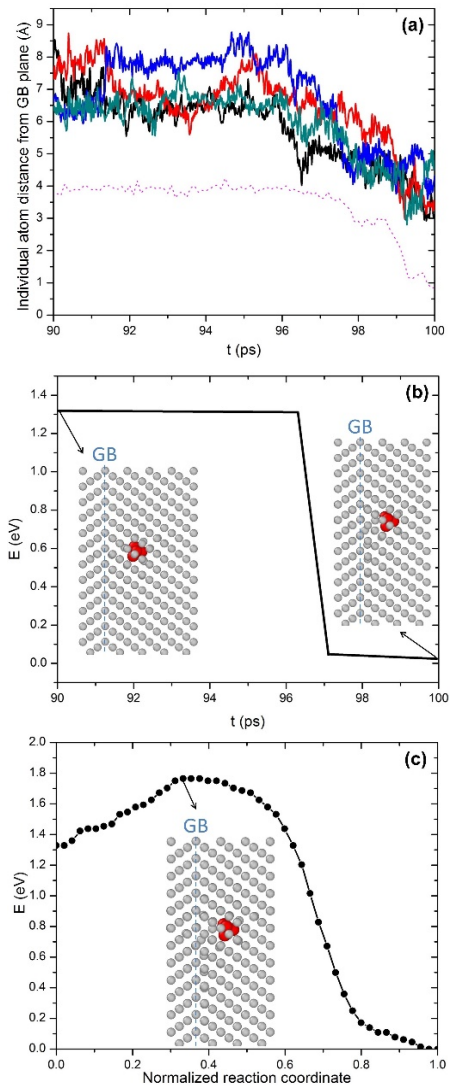

Fig. 6. Analysis of a representative MD trajectory capturing the dominant He_4 cluster TM reaction, W + He_4 → He_4-V (l=3) + W_{GB}, near the Σ3<111>{121} symmetric tilt GB in tungsten, with the vacancy of the He_4-V complex forming on the 3rd atomic layer from the GB plane. (a) Evolution of the distance from the GB plane of all four He atoms of the He_4 cluster (solid lines) and of the W atom displaced substantially from its original lattice position (dotted line) during the TM reaction, showing the formation of a W interstitial atom in the form of an extended W interstitial complex on the GB, W_{GB}. (b) Energy evolution along the quenched MD trajectory during the trap mutation reaction. (c) Energy landscape along the optimal reaction pathway. In the inserted configurations in (b) and (c), silver and red spheres denote W and He atoms, respectively, and the blue dashed vertical line indicates the GB plane.

content, which are expected to influence the amount of hydrogen re-cycling and tritium retention in fusion tokamaks. This work has been published as an article in the *Journal of Applied Physics* [6].

6. *Dynamics of Small Mobile Helium Clusters Near a Symmetric Tilt Grain Boundary of Plasma-Exposed Tungsten*

We have carried out a systematic atomic-scale analysis of small helium cluster dynamics near a Σ3<111>{121} symmetric tilt grain boundary (GB) in tungsten based on molecular-dynamics (MD) simulations according to a reliable interatomic interaction potential. We have found that small, mobile helium clusters (He_n, $1 \leq n \leq 7$) in the near-GB region are attracted to the GB due to an elastic cluster-GB interaction force. Moreover, as the clusters drift toward the GB, cluster trap mutation (TM) reactions in the near-GB region are activated at rates much higher than those in the bulk of the material's grains; the analysis of a representative TM reaction for the He_4 cluster is shown in Fig. 6. This near-GB cluster dynamics has significant effects on the near-GB defect structures and the amount of helium retained in the material upon plasma exposure. Each TM reaction generates a tungsten vacancy, which traps helium by forming an immobile helium-vacancy complex, and an interstitial tungsten atom in the form of an extended tungsten interstitial complex on the GB. This interstitial configuration is characterized by mobility that depends on the location where the TM reaction occurs: it is immobile when the vacancy produced by the TM reaction is located a few lattice planes away from the GB plane and highly mobile along a specific direction when the produced vacancy is located on the GB. The latter mechanism initiates a potentially fast migration path for W atoms along the GB toward a free surface, which may influence significantly the surface morphology of plasma-exposed tungsten. This work has been published as an article in a special issue (on Plasma-Materials Interactions) of

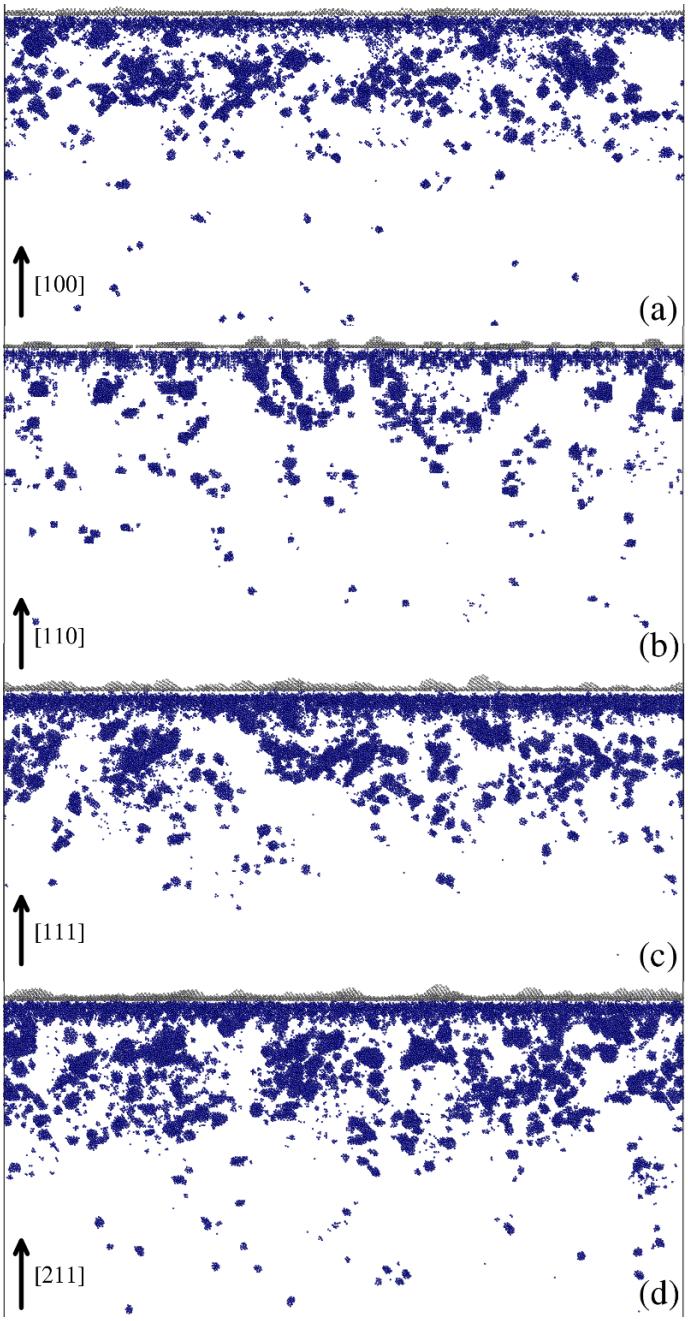

Fig. 7. Distribution of He atoms (colored blue) in tungsten from large-scale MD simulations of clustering and surface segregation of He atoms implanted in W, at 933 K and an impingement energy of 100 eV, near (a) W(100), (b) W(110), (c) W(111), and (d) W(211) free surfaces; W adatoms (colored gray) formed in near-surface trap mutation and sub-surface loop-punching processes also are shown. The width of each image is 50 nm. Each image does not depict a cross section but rather a side view through the entire simulation cell.

Fusion Science and Technology [7].

7. *Helium Segregation and Transport Behavior near* <100> *and* <110> *Symmetric Tilt Grain Boundaries in Tungsten*

We have carried out a systematic atomistic modeling study of small helium cluster behavior near tungsten symmetric tilt grain boundaries. This behavior was studied qualitatively by molecular-dynamics simulations and quantitatively by molecular-statics simulations combined with elastic inclusion theory. The sink strength is used to describe the magnitude of the clusters' attraction to the grain boundary. We find that small helium clusters show impeded transport behavior relative to the bulk around all types of grain boundaries, including low-angle, high-angle, low-Sigma-value, and high-Sigma-value grain boundaries. Helium clusters tend to become trapped near, but typically not directly on, the grain boundary plane. Both the distance between the helium cluster and the grain boundary when the cluster first becomes immobilized and the sink strength are correlated with helium cluster size, grain boundary formation energy, grain boundary tilt angle, excess volume, and other aspects of grain boundary structure. We expect similar impeded transport behavior for other types of grain boundaries and in other metals, because helium is effectively insoluble in most materials and has a similar interstitial-based diffusion mechanism in most metals. This work has been published as an article in the *Journal of Applied Physics* [8].

8. *Helium Segregation on Surfaces of Plasma-Exposed Tungsten*

We have conducted a hierarchical multi-scale modeling study of implanted helium segregation on surfaces of tungsten, considered as a plasma facing component in nuclear fusion reactors. We employed a hierarchy of atomic-scale simulations based on a reliable interatomic interaction potential, including molecular-statics simulations to understand the origin of helium surface segregation, targeted molecular-dynamics (MD) simulations of near-surface cluster reactions, and large-scale MD simulations of implanted helium evolution in plasma-exposed tungsten; representative large-scale MD simulation results are shown in Fig. 7. We have found that small, mobile He_n ($1 \leq n \leq 7$) clusters in the near-surface region are attracted to the surface due to an elastic interaction force that provides the thermodynamic driving force for surface segregation. This elastic interaction force induces drift fluxes of these mobile He_n clusters, which increase substantially as the migrating clusters approach the surface, facilitating helium segregation on the surface. Moreover, the clusters' drift toward the surface enables cluster reactions, most importantly trap mutation, in the near-surface region at rates much higher than in the bulk material. These near-surface cluster dynamics have significant effects on the surface morphology, near-surface defect structures, and the amount of helium retained in the material upon plasma exposure. We have integrated the findings of such atomic-scale simulations into a properly parameterized and validated spatially dependent, continuum-scale reaction-diffusion cluster dynamics model, capable of predicting implanted helium evolution, surface segregation, and its near-surface effects in tungsten. This cluster-dynamics model sets the stage for development of fully atomistically informed coarse-grained models for computationally efficient simulation predictions of helium surface segregation, as well as helium retention and surface morphological evolution, toward optimal design of plasma facing components. This work has been published as a research article in a special issue (on Surface Segregation) of the *Journal of Physics: Condensed Matter* [9].

9. *Modeling Helium Segregation to the Surfaces of Plasma-Exposed Tungsten as a Function of Temperature and Surface Orientation*

We have provided a description of the dependence on surface crystallographic orientation and temperature of the segregation of helium implanted with energies consistent with low-energy plasma exposure to tungsten surfaces. This is a multi-scale modeling description based on a hierarchical approach to scale bridging that incorporates atomistic studies according to a reliable interatomic potential to parameterize a spatially dependent drift-diffusion-reaction cluster-dynamics code. We have performed an extensive set of molecular-dynamics (MD) simulations at 933 K and/or 1200 K to determine the probabilities of desorption and modified trap mutation which occurs as small, mobile He_n ($1 \leq n \leq 7$) clusters diffuse from the near-surface region towards surfaces of varying crystallographic orientation due to an elastic interaction force that provides the thermodynamic driving force for surface segregation. These near-surface cluster dynamics have significant effects on the surface morphology, near-surface defect structures, and the amount of helium retained in the material upon plasma exposure, for which we have developed an extensive MD database of cumulative evolution during high-flux helium implantation at 933 K, which we have compared to our properly parameterized cluster-dynamics model; such representative comparisons are shown in Fig. 8. We have then used this validated model to evaluate the effects of temperature on helium retention and sub-surface helium

clustering. This work has been published as an article in a special issue (on Plasma-Materials Interactions) of *Fusion Science and Technology* [10].

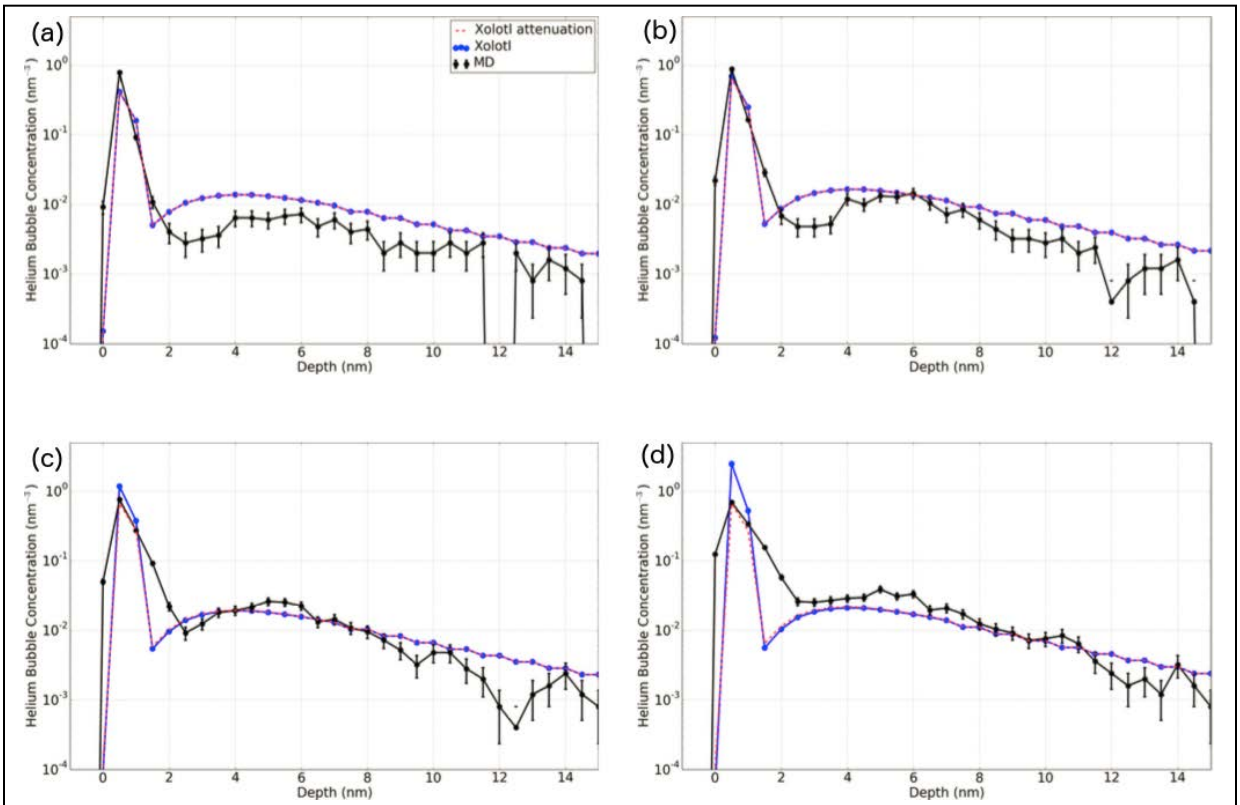

Fig. 8. Comparison of MD simulation results (black solid circles with accompanying error bars from statistical analysis of the MD trajectories) with Xolotl predictions without (blue solid circles) and with (red dotted lines) attenuation of near-surface reaction rates for helium bubble concentration as a function of depth below a W(111) surface at 933 K during 100-eV helium implantation at a flux of about 4×10^{25} $m^{-2}s^{-1}$, with a helium implantation fluence of (a) 5×10^{18} m^{-2}, (b) 1.0×10^{19} m^{-2}, (c) 2.0×10^{19} m^{-2}, and (d) 4.0×10^{19} m^{-2}.

10. *Large-Scale Atomistic Simulations of Low-Energy Helium Implantation into Tungsten Single Crystals*

We have conducted large-scale molecular-dynamics simulations of post-implantation helium behavior in plasma-facing tungsten single crystals, which have revealed orientation-dependent depth profiles, surface evolution patterns, and other crystallographic and diffusion-related characteristics of helium behavior in tungsten during the first microsecond. The flux of implanted helium atoms studied, $\Gamma \approx 4{\times}10^{25}$ m^{-2} s^{-1}, is about one order of magnitude larger than that expected in ITER, the experimental fusion reactor currently being constructed in France. With simulation times on the order of 1 μs, these results serve to discover the mechanisms involved in surface evolution as well as to serve as benchmarks for coarse-grained simulations such as kinetic Monte Carlo and continuum-scale drift-reaction-diffusion cluster dynamics simulations. The findings of our large-scale simulations are significant due to diminished finite-size effects and the longer times reached (corresponding to higher fluences). Specifically, our findings are drastically different from findings published previously in the literature for (001) surfaces under a helium flux of $\Gamma \sim 10^{28}$ m^{-2} s^{-1}, which is typical of smaller size and shorter time

atomistic simulations. In particular, this study highlights the atomic-scale materials processes relevant to helium entrapment and transport in metals, which have implications not only for nuclear fusion-relevant processes, but also helium-induced embrittlement in irradiated materials such as hospital equipment and fission reactor materials. This work has been published as an article in *Acta Materialia* [11].

11. *Benchmarks and Tests of a Multidimensional Cluster Dynamics Model of Helium Implantation in Tungsten*

We have carried out a hierarchical multi-scale modeling study of implanted helium segregation near grain boundaries of tungsten. We have extended our spatially dependent cluster dynamics model to two spatial dimensions in order to take into account the biased drift of mobile helium clusters toward the grain boundaries observed in atomic-scale simulations. With this extended cluster-dynamics model, we have been able to reproduce the results from large-scale molecular-dynamics simulations both near and away from the grain boundaries at low fluence. We proposed and verified that the sink (surface and grain boundary) strengths are attenuated by the increasing concentration of helium clusters at high fluence. This cluster-dynamics model continues to set the stage for development of fully atomistically-informed, coarse-grained models for computationally efficient predictions of helium retention and surface morphological evolution, advancing progress toward the goal of efficient and optimal design of plasma-facing components. This work has been published as an article in a special issue (on Plasma-Materials Interactions) of *Fusion Science and Technology* [12]. Current work focuses on improving the predictive capabilities of this model by full incorporation of the atomistic database of near-surface and near-GB helium cluster reaction probabilities and fine tuning of the segregation strength and reaction rate attenuation procedure.

12. *Thermal Conductivity of Tungsten: Effects of Plasma-Related Structural Defects from Molecular-Dynamics Simulations*

We have conducted a systematic study on the lattice thermal conductivities of tungsten single crystals containing nanoscale-sized pores or voids and helium (He) nanobubbles as a function of void/bubble size and gas pressure in the He bubbles based on molecular-dynamics simulations. For reference, we calculated lattice thermal conductivities of perfect tungsten single crystals along different crystallographic directions at room temperature and found them to be about 10% of the overall thermal conductivity of tungsten with a weak dependence on the heat flux direction. The presence of nanoscale voids in the crystal causes a significant reduction in its lattice thermal conductivity, which decreases with increasing void size. Filling the voids with He to form He nanobubbles and increasing the bubble pressure leads to further significant reduction of the tungsten lattice thermal conductivity, down to ~20% of that of the perfect crystal. The anisotropy in heat conduction remains weak for tungsten single crystals containing nanoscale-sized voids and He nanobubbles throughout the pressure range examined. Analysis of the pressure and atomic displacement fields in the crystalline region that surrounds the He nanobubbles reveals that the significant reduction of tungsten lattice thermal conductivity in this region is due to phonon scattering from the nanobubbles, as well as lattice deformation around the nanobubbles and formation of lattice imperfections at higher bubble pressure. This work has been published as an article in *Applied Physics Letters* [13].

References:

1. B. D. Wirth, K. D. Hammond, S. I. Krasheninnikov, and D. Maroudas, "Challenges and Opportunities of Modeling Plasma Surface Interactions in Tungsten Using High Performance Computing," *Journal of Nuclear Materials* **463**, 30-38 (2015) [DOI: 10.1016/j.jnucmat.2014.11.072].

2. D. Maroudas, X. Han, and S. C. Pandey, "Design of Semiconductor Ternary Quantum Dots with Optimal Optoelectronic Function," *AIChE Journal* **59**, 3223-3236 (2013) [DOI: 10.1002/aic.14118].
   - **Invited article** for special *AIChE J*. issue on *Tribute to Founders*: *Neal R. Amundson*

3. L. Hu, K. D. Hammond, B. D. Wirth, and D. Maroudas, "Interactions of Mobile Helium Clusters with Surfaces and Grain Boundaries of Plasma-Exposed Tungsten," *Journal of Applied Physics* **115**, Article No. 173512, 8 pages (2014) [DOI: 10.1063/1.4874675].

4. L. Hu, K. D. Hammond, B. D. Wirth, and D. Maroudas, "Dynamics of Small Mobile Helium Clusters near Tungsten Surfaces," *Surface Science* **626**, L21-L25 (2014) [DOI: 10.1016/j.susc.2014.03.020].

5. K. D. Hammond, L. Hu, D. Maroudas, and B. D. Wirth, "Helium Impurity Transport on Grain Boundaries: Enhanced or Inhibited?," *Europhysics Letters* **110**, Article No. 52002, 6 pages (2015) [DOI: 10.1209/0295-5075/110/52002].

6. L. Hu, K. D. Hammond, B. D. Wirth, and D. Maroudas, "Molecular-Dynamics Analysis of Mobile Helium Cluster Reactions near Surfaces of Plasma-Exposed Tungsten," *Journal of Applied Physics* **118**, Article No. 163301, 12 pages (2015) [DOI: 10.1063/1.4933393].

7. L. Hu, K. D. Hammond, B. D. Wirth, and D. Maroudas, "Dynamics of Small Mobile Helium Clusters Near a Symmetric Tilt Grain Boundary of Plasma-Exposed Tungsten," *Fusion Science and Technology* **71**, 36-51 (2017) [DOI: 10.13182/FST16-105].

8. Z. Yang, L. Hu, D. Maroudas, and K. D. Hammond, "Helium Segregation and Transport Behavior near <100> and <110> Symmetric Tilt Grain Boundaries in Tungsten," *Journal of Applied Physics* **123**, Article No. 225104, 12 pages (2018) [DOI: 10.1063/1.5026617].

9. D. Maroudas, S. Blondel, L. Hu, K. D. Hammond, and B. D. Wirth, "Segregation of Helium on Surfaces of Plasma-exposed Tungsten," *Journal of Physics*: *Condensed Matter* **28**, Article No. 064004, 13 pages (2016) [DOI: 10.1088/0953-8984/28/6/064004].
   - **Invited research article** for special issue on *Surface Segregation*.

10. S. Blondel, L. Hu, K. D. Hammond, D. Maroudas, and B. D. Wirth, "Modeling Helium Segregation to the Surfaces of Plasma-Exposed Tungsten as a Function of Temperature and Surface Orientation," *Fusion Science and Technology* **71**, 22-35 (2017) [DOI: 10.13182/FST16-112].

11. K. D. Hammond, S. Blondel, L. Hu, D. Maroudas, and B. D. Wirth, "Large-Scale Atomistic Simulations of Low-Energy Helium Implantation into Tungsten Single Crystals," *Acta Materialia* **144**, 561-578 (2018) [DOI: 10.1016/j.actamat.2017.09.061].

12. S. Blondel, D. E. Bernholdt, K. D. Hammond, L. Hu, D. Maroudas, and B. D. Wirth, "Benchmarks and Tests of a Multidimensional Cluster Dynamics Model of Helium Implantation in Tungsten," *Fusion Science and Technology* **71**, 84-92 (2017) [DOI: 10.13182/FST16-109].

13. L. Hu, B. D. Wirth, and D. Maroudas, "Thermal Conductivity of Tungsten: Effects of Plasma-Related Structural Defects from Molecular-Dynamics Simulations," *Applied Physics Letters* **111**, Article No. 081902, 5 pages (2017) [DOI: 10.1063/1.4986956].